



Li, S., Yu, X., Sun, Y., Jin, L. and Xia, Z. (2022) An interference-reducing precoding for SCMA multicast design based on complementary sequences. *IEEE Transactions on Broadcasting*, (doi: 10.1109/TBC.2022.3201637).

There may be differences between this version and the published version. You are advised to consult the publisher's version if you wish to cite from it.

<https://eprints.gla.ac.uk/278490/>

Deposited on: 5 September 2022

Enlighten – Research publications by members of the University of Glasgow
<https://eprints.gla.ac.uk>

An Interference-reducing Precoding for SCMA Multicast Design Based on Complementary Sequences

Shufeng Li, *Member, IEEE*, Xin Yu, Yao Sun, *Senior Member, IEEE*, Libiao Jin, *Member, IEEE*, and Zhiping Xia

Abstract—In a multi-group multicast sparse code multiple access (SCMA) system, one base station multicasts common messages to multiple multicast groups via different code books. To accommodate more user terminals (UTs), traditional multicast systems have multiple transmitters, each of which works in one-to-many mode. In this way, each UT is subject to inter-transmitter interference. Considering the high degrees of freedom for transmitting and receiving, it is difficult to separate the desired signal from interference signals. Therefore, an interference-reducing precoding scheme is required to ensure the reliability of SCMA multicast communication system. For the SCMA multicast system design, we present three necessary conditions that the interference-reducing matrix should satisfy. Then, the precoding matrix satisfying the three necessary conditions simultaneously is designed by utilizing the complementary sequences (CS) and complete complementary sequences (CCS). In this context, we consider two scenarios with different transmission modes (single-cell and multiple-cell) and different precoding schemes (based on CS and CCS). Simulation results show that proposed transmission schemes can significantly reduce the bit error rate of multicast groups while ensuring the communication throughput, and behave a superior performance over other alternatives. Moreover, theoretical and simulation results also prove that the proposed precoding vectors have perfect average power radiation and omnidirectional coverage performance.

Index Terms—SCMA, multicast, complementary sequences, complete complementary sequences, precoding.

I. INTRODUCTION

IN order to accommodate massive number of users and to meet the business requirements of applications such as content distribution and emergency alerts, non-orthogonal multiple access (NOMA) technology transmit multiple information streams on overlapping wireless resources in the time/frequency/code domains to increase transmission throughput and improve user access fairness [1]–[3]. In the existing NOMA technologies, sparse code multiple access

(SCMA) is a strategy based on the code domain [4]. In SCMA systems, several symbols in user’s complex space are diffused into sparse code words which are chosen from a pre-defined code book and the sparse code words are superimposed and sent by using marker vectors. In addition, with the development of multicast broadcasting technology in cellular cells, wireless multicast technology can transmit the same data to all members in the same multicast group [5]–[7]. Once the base station (BS) has loaded the service information onto the time-frequency resource, all users in the same multicast group can receive service data from the time-frequency resource. In this way, it enables multiple users to share the same time-frequency resource and increases the number of users that can be served per unit of spectrum resource [8]–[10].

In addition, many previous works on SCMA focus on the analysis of unicast performance, in which the information sent by BS can only be received by one user. Early studies on SCMA mainly focused on the unicast technology, namely, uplink and downlink propagation of SCMA, the design of the codebook, and the complexity of multi-user detection technology at the receiver. For example, in terms of SCMA system design, work [11] not only designed the uplink SCMA system model, but also proposed coding and multi-user detection methods, and verified the performance of the SCMA uplink and downlink systems through simulations. However, only two transmit antennas and two receive antennas are considered for the case in this MIMO-SCMA system, and the reliability and BER performance results are not good if it is applied directly to a massive MIMO scenario. In work [12], the authors propose a downlink multi-dimensional spatial time block code multiple-input multiple-output SCMA (MSTBC-MIMO-SCMA) scheme, which is based on the extension of STBC for conventional MIMO systems. This MSTBC-assisted downlink MIMO-SCMA system model can achieve full rate and full diversity, but its BER performance is not satisfactory, especially if this model is directly applied to the massive MIMO multicast scenario without considering the complex interference in the multicast environment. Work [13] designed a new MPA-based detector for downlink MIMO-SCMA systems for the first time, and work [14] proposed a novel graph-based low-complexity multi-user detection algorithm for SCMA systems. Although it was possible to combine the features of MIMO and SCMA to design a new receiver-side detector, this research is still stuck on unicast technology.

In conventional multicast schemes, reliability of commun-

Manuscript received XX XX, 20XX; revised XX XX, 20XX. This work was supported by Fundamental Research Funds for the Central Universities under Grant: CUC210B032. (*Corresponding author: Libiao Jin.*)

Shufeng Li and Xin Yu are with the State Key Laboratory of Media Convergence and Communication, Communication University of China, Beijing 100024, China (e-mail: lishufeng@cuc.edu.cn; emillyu98@cuc.edu.cn).

Yao Sun is with James Watt School of Engineering, University of Glasgow, Glasgow, G12 8QQ, U.K. (e-mail: Yao.Sun@glasgow.ac.uk).

Libiao Jin is with the State Key Laboratory of Media Convergence and Communication, Communication University of China, Beijing 100024, China (e-mail: libiao@cuc.edu.cn).

Zhiping Xia is with Academy of Broadcasting Science, Beijing 100024, China (e-mail: xiazhiping@abs.ac.cn).

ication depends on how to separate the required signal from many interference signals. In order to tackle this problem, the authors in [15] proposed an interference subspace alignment algorithm, which can decrease the dimension of the interference subspace. The interference subspace alignment algorithm directly aligns the interference subspace spanned by the $T - N$ transmitters within that spanned by the residual N transmitters. In addition, studies of multicast communication have also emphasized on interference coordination. In [16], a dynamic power control scheme is proposed to mitigate the interference from Device-to-Device (D2D) multicast transmission to cellular networks. This scheme determine the upper bound of transmit power based on the location of BSs and areas of adjacent cells from the coverage area of D2D multicast group.

From the above elaboration, both SCMA technology and multicast transmission technology can alleviate the shortage of spectrum resources in wireless networks with high spectrum efficiency, providing the possibility to meet the demand of ultra-high density access. Therefore, SCMA technology and multicast transmission technology are jointly proposed to handle ultra-high-definition video streaming and provide services that meet the end user's perceived quality requirements [17].

In contrast to SCMA in unicast networks, the application of SCMA to multicast networks is still in its infancy. For multicast systems, the performance is generally considered to be determined by the receiver with the worst channel gain in the multicast group. As a result, the complete performance analysis of unicast SCMA cannot be directly applied to multicast SCMA systems. Based on this fact, literature [18] proposes an analytical method to obtain a tight upper bound on the bit error rate (BER) of a multicast SCMA system. Another important observation is that both SCMA and wireless multicast can alleviate the shortage of spectrum resources in 5G and Internet of Things (IoT) networks. Work [19] introduced SCMA layered multicast in IoT systems to take advantage of its advantages to expand network capacity, which can also achieve higher spectral efficiency and link utilization.

Considering the limitations of these existing algorithms stated above, we exploit the idea of complementary codes based scheme to further address the interference problems in SCMA multicast systems. In this paper we investigate SCMA under a multiple-multicast network with the objective of reducing the inter-transmitter interference. First, the precoding matrix needs to guarantee omnidirectional transmission. Because the public channel needs to serve all users in the cell, including active users, inactive users, users close to the BS, and users located at the edge of the cell. For multicast systems, the performance is generally considered to be determined by the receiver with the worst channel gain in the multicast group. A reasonable method is to make the transmitting signal of the BS have spatial omnidirectional characteristics so as to cover the whole cell. In this case, no matter where the user is located, it can obtain a reliable signal-to-noise ratio (SNR). As a wireless communication system, power efficiency also needs to be considered, such as the efficiency of transmitting antenna power amplifiers (PAs). In a massive MIMO system, due to the small size of the antenna array, the transmitting

antenna PA also decreases correspondingly and is limited to the linear working range, that is, the transmitting power of each antenna cannot exceed a maximum value, otherwise the working efficiency of the antenna PA will be reduced. To make full use of the full PA in the BS, the average power of the transmitted signal at each antenna is required to be equal. In addition, we also expect the omnidirectional precoding matrix to maximize the reachable traversal rate. The main contributions of this paper are summarized as follows.

- We introduce a precoding design into the SCMA multicast system, and two precoding transmission schemes are considered. We first present necessary requirements that the precoding matrix should satisfy under the multicast transmission. Then we derive that such a precoding matrix can be constructed based on the complementary sequences (CS) and the complete complementary sequences (CCS). The resultant CS-based and CCS-based precoding schemes are therefore very suitable for SCMA multicast design because of some linear constraints on the auto- and cross-correlation of the precoding vectors.

- For the single-cell SCMA multicast transmission, the precoding matrix which constructed based on CS and CCS can be applied in different multicast groups to realize reliable cell-wide coverage, equal average power on each antenna and achievable ergodic rate maximization, thus guaranteeing the message coverage for each user in the same multicast group, especially for the weak users at the edge of the cell.

- For the multi-cell SCMA multicast transmission, the precoding matrix which constructed based on CS and CCS can limit the inter-group inference, especially for users at the overlapping boundaries of multiple cells. In addition, we theoretically analyze that the downlink pilot overhead can be significantly reduced, thus reducing the complexity of the whole algorithm. The multi-cell system model is promising and can be well applied to various scenarios, such as the multi-cell downlink data transmission, and the distributed massive antenna array, single frequency network, etc.

The remainder of this paper is organized as follows. Section II describes the channel model and system model of multiple-multicast network employing SCMA. Section III presents the formulation of the proposed precoding matrix construction and the method of constructing CCS. Section IV details the application of proposed CS and CCS based precoding scheme in SCMA multicast system. The numerical results are presented in Section V. Finally, this paper is concluded in Section VI.

Notations: Bold upper-case and lower-case letters represent matrices and column vectors, respectively; $(\cdot)^{-1}$, $(\cdot)^T$ and $(\cdot)^H$ denote inversion, transpose, and conjugate transpose, respectively. $\mathbf{A}(i, j)$, $\mathbf{A}(:, j)$ and $\mathbf{A}(i, :)$ respectively denote the (i, j) -th complex element, j -th column vector and i -th row vector of matrix \mathbf{A} , and $|\mathbf{A}(i, j)|$ is the amplitude; $diag\{\mathbf{a}\}$ denotes the diagonal matrix with vector \mathbf{a} as the diagonal; $[\mathbf{a}]_m$ denotes the m -th diagonal element of vector \mathbf{a} ; $\|\cdot\|_F$ represents the Frobenius norm; \otimes denotes the operation of Kronecker product; $\mathcal{CN}(0, \sigma^2)$ is the complex Gaussian distribution with

mean 0 and the variance σ^2 ; $\mathbb{D}^{l \times l}$ and $\mathbb{C}^{m \times n}$ describe a real diagonal matrix of dimension $l \times l$ and a complex matrix of dimension $m \times n$, respectively; $\text{tr}(\cdot)$ and $\text{Re}(\cdot)$ indicate the trace and real part taking operators, respectively; $\Re(\cdot)$ denotes imaginary component of a complex number. Furthermore, we use \mathbf{I}_N to denote the $N \times N$ identity matrix. $\mathbf{0}_N$ and $\mathbf{1}_N$ represent $N \times N$ matrices whose elements all equal zero and one, respectively. Expectation operator is denoted by $E\{\cdot\}$. The x value that maximizes $f(x)$ is expressed as $\arg \max_x \{f(x)\}$. Finally, $P\{\cdot\}$ represents the probability of occurrence,

II. SYSTEM MODEL

A. Rayleigh Flat-fading Channel Model

We consider the downlink of a multi-user cell where a BS is equipped with a uniform linear array (ULA) of M_{BS} antennas and simultaneously communicates with N_{MS} single-antenna users [20]. In this paper, we consider a generic channel model $\mathbf{H} \in M_{BS} \times 1$ which denotes the channel vector between the BS and the k -th user, and assume that the channel is a Rayleigh flat fading channel. In Rayleigh channel, \mathbf{H} follows a cyclic symmetric complex Gaussian distribution

$$\mathbf{H} \sim \mathcal{CN}(\mathbf{0}, \mathbf{R}). \quad (1)$$

According to the conclusions of [21], the covariance matrix \mathbf{R} of the channel can be expressed as

$$\mathbf{R} = \beta \cdot \int_{-\frac{\pi}{S}}^{\frac{\pi}{S}} \mathbf{v}(\theta) \mathbf{v}(\theta)^H p(\theta) d\theta, \quad (2)$$

where $\beta = 1$ represents the large-scale fading coefficient, S represents the number of sectors, $\mathbf{v}(\theta) = [1, e^{-j2\pi d \sin \theta / \lambda}, \dots, e^{-j2\pi(N_{BS}-1)d \sin \theta / \lambda}]^T$ represents the array response vector of the ULA, θ denotes the angle between the direct path and the direction normal to the array, λ denotes the carrier wavelength, d denotes the neighboring antenna spacing and $p(\theta)$ denotes the power azimuth spectrum (PAS) of the multipath channel, which follows different distributions.

When the number of antennas at the BS is sufficiently large, the covariance matrix of the channel has the following eigenvalue decomposition form [22]

$$\mathbf{R} \rightarrow \mathbf{F}_{M_{BS}}^H \mathbf{\Lambda} \mathbf{F}_{M_{BS}}, \quad (3)$$

where the eigenvector matrix $\mathbf{F}_{M_{BS}}$ is a M_{BS} point normalized DFT matrix and the diagonal elements on the diagonal matrix $\mathbf{\Lambda} = \text{diag}\{\Lambda_0, \Lambda_1, \dots, \Lambda_{M_{BS}-1}\}$ of eigenvalues are asymptotically identically distributed with the PAS discrete sampling values [23].

Therefore, the channel can be approximated as

$$\mathbf{H} \sim \mathcal{CN}\left(\mathbf{0}, \mathbf{F}_{M_{BS}}^H \mathbf{\Lambda} \mathbf{F}_{M_{BS}}\right). \quad (4)$$

We use (4) as the most basic channel model in this paper to discuss the following analysis and design.

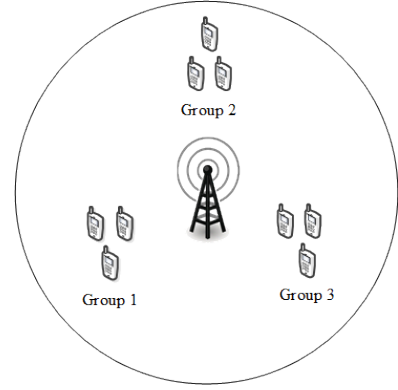


Fig. 1. Single-cell Multicast Model.

B. SCMA Multicast System Model

In this paper, we analyze the received signal of a general multicast system in order to compare it with SCMA multicast system. In the massive MIMO multicast downlink system, we assume that the number of BS is N_{BS} . Each BS is equipped with M_{BS} antennas, and simultaneously communicates with N_{MS} users, each equipped with single antenna. Then the signal received of the k -th user can be expressed as

$$\mathbf{y}_k = \mathbf{H}_k^H \mathbf{W}_k \mathbf{x}_k + \sum_{j \neq k}^{N_{MS}} \mathbf{H}_j^H \mathbf{W}_j \mathbf{x}_j + \mathbf{n}, \quad (5)$$

where $\mathbf{H}_k \in \mathbb{C}^{M_{BS} \times 1}$ is the downlink channel vector for the k -th user and the BS, $\mathbf{W}_k \in \mathbb{C}^{M_{BS} \times N_w}$ is the precoding matrix for the k -th user, \mathbf{x}_k is the low-dimensional transmission signal, and \mathbf{n} is the additive Gaussian noise vector.

Single-cell multicast model: there is only one BS in the cell, the BS only communicates with one multicast group during a time slot as Fig.1 shown. All users in a multicast group receive the same information. The wireless system is faced with complex and bad wireless channels, because of the existence of fading, noise, multipath and so on, and multicast service users will also have the difficulty of receiving failure. We use (i, j) to represent the i -th user in cell j . The signal received by the i -th user in cell j can be expressed as

$$\mathbf{y}_{i,j} = \mathbf{H}_{(i,j),j}^H \mathbf{W}_j \mathbf{x}_j + \mathbf{n}. \quad (6)$$

where $\mathbf{H}_{(i,j),j}$ is the downlink channel matrix between the BS in the j -th cell and (i, j) -user. The single-cell model is suitable for the scenario where the number of near and far users is not equal, and the whole time period is divided into multiple time slots, where the dynamic pairing scheme is implemented in different time slots. Thus, the sub-channel resources are fully utilized, and the number of access users can be increased.

Multi-cell multicast model: each cell is equipped with a BS, and J different multicast groups communicating simultaneously in the same time slot as Fig.2 shown. We focus on the case where there is only one multicast group in each cell. The multicast information of different multicast groups is different. This may cause interference to users at the margin of the cell. Assume the number of cell is J , thus the signal received by the i -th user in cell j can be expressed as [24]

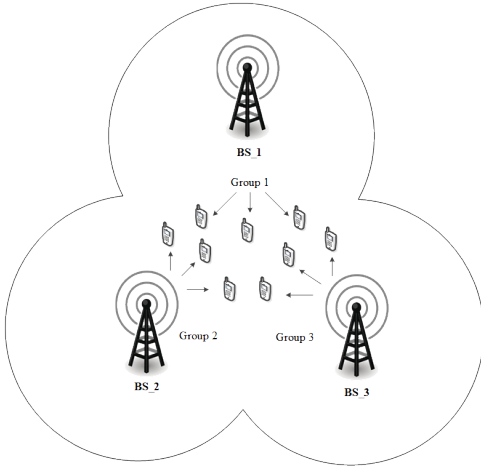


Fig. 2. Multi-cell Multicast Model.

$$\mathbf{y}_{i,j} = \mathbf{H}_{(i,j),j} \mathbf{W}_j \mathbf{x}_j + \sum_{m \neq j}^J \mathbf{H}_{(i,j),m} \mathbf{W}_m \mathbf{x}_m + \mathbf{n}, \quad (7)$$

where where $\mathbf{H}_{(i,j),m}$ is the downlink channel matrix between the BS in the m -th cell and (i,j) -user, \mathbf{W}_j is the unique precoding vector enjoyed by the cell j .

Assume that in the SCMA multicast system, J groups of users share K orthogonal time-frequency resources, the number of users in the m -th multicast group is J_m . Each multicast group occupies one codebook and that no other user group shares this codebook. On the receiver side, after precoding and fading the channel, the received signal for the i -th multicast user in the multicast j -th group can be expressed as

$$\mathbf{y}_{i,j} = \begin{cases} \text{diag} \left(\mathbf{H}_{(i,j),j} \mathbf{W}_j \right) \mathbf{x}_j + \mathbf{n}, & (8a) \\ \text{diag} \left(\mathbf{H}_{(i,j),j} \mathbf{W}_j \right) \mathbf{x}_j \\ + \sum_{m \neq j}^J \text{diag} \left(\mathbf{H}_{(i,j),m} \mathbf{W}_m \right) \mathbf{x}_m + \mathbf{n}. & (8b) \end{cases}$$

In (8a), $\mathbf{y}_{i,j}$ is the superposition of target user information and noise in single-cell multicast model, in (8b), $\mathbf{y}_{i,j}$ is the received signal matrix with all multicast groups information and noise superimposed in multi-cell multicast model, \mathbf{x}_j is the code word of the j -th multicast group, $\mathbf{H}_{(i,j),m} \in \mathbb{C}^{M_{BS} \times N_{MS}}$ is the downlink channel matrix between the BS in the m -th cell and (i,j) -user and $\mathbf{W}_j \in \mathbb{C}^{M_{BS} \times K}$ is the precoding matrix. For fair comparisons, the transmit power of each multicast group in the SCMA network is set to be equal.

III. PROBLEM FORMULATION

Assume that the low-dimensional transmitted signals in the precoding domain are $\mathbf{x} = [x_1, \dots, x_{N_W}]^T$ and satisfy $E\{\mathbf{x}\} = \mathbf{0}$ and $E\{\mathbf{x}\mathbf{x}^H\} = \mathbf{I}_{N_W}$, which means the low-dimensional transmitted signals are mutually independent sequences of symbols. To ensure that the total transmit power

of the BS is constant, the precoding matrix \mathbf{W} needs to satisfy equation $\text{tr}(\mathbf{W}\mathbf{W}^H) = 1$. It is worth noting that the precoding matrix in this paper should be channel specific independent.

A. Three Requirements of The Precoding

We derive three basic requirements for the precoding matrix in terms of omnidirectionality of the signal in the angular domain, PA utilization and maximization of the rate of information traversed under the independent identically distributed (i.i.d.) channel.

Although massive MIMO communication systems are capable of providing superior quality signal transmission services to specific receiving terminals by means of beamforming, full coverage of all service areas is required for a qualified signal transmission system for the transmission of the common signal. Consequently, the precoding matrix needs to have equivalent transmit power in the angular domain, i.e., to ensure the omnidirectionality of the transmitted signal. The transmitted signal in the angular domain is

$$s(\theta) = \frac{1}{\sqrt{M_{BS}}} \sum_{m=1}^{M_{BS}} [\mathbf{W}\mathbf{x}]_m e^{j2\pi\Delta(m-1)\sin\theta}, \theta \in [-\pi/K, \pi/K]. \quad (9)$$

Let $\Delta = \frac{1}{2\sin(\pi/K)}$, $\omega = -\Delta \sin\theta$, the above equation can be expressed as

$$\tilde{s}(\omega) = \frac{1}{\sqrt{M_{BS}}} \sum_{m=1}^{M_{BS}} [\mathbf{W}\mathbf{x}]_m e^{j2\pi(m-1)\omega}, \omega \in [-1/2, 1/2], \quad (10)$$

which means that the transmitted signal in the angular domain is essentially a discrete time Fourier transform of the transmitted signal in the physical domain. In order to ensure that all user terminals (UTs) in the control area of the communication system achieve an equivalent quality-of-service, an intuitive consideration is to ensure that the average transmit power is satisfied within $\omega \in [-1/2, 1/2]$, to ensure that

$$P(\omega) = \rho \cdot E \left\{ |\tilde{s}(\omega)|^2 \right\} = \rho \cdot \mathbf{f}_\omega \mathbf{W}\mathbf{W}^H \mathbf{f}_\omega^H \quad (11)$$

is independent of ω . To guarantee transmission omnidirectionality in the continuous angular domain, the precoding matrix needs to satisfy

$$\mathbf{f}_\omega \mathbf{W}\mathbf{W}^H \mathbf{f}_\omega^H = \text{const}, \quad (12)$$

where $\mathbf{f}_\omega = \frac{1}{\sqrt{M_{BS}}} [1, e^{-j\omega}, \dots, e^{-j(M_{BS}-1)\omega}]$ is the DTFT transform vector. After satisfying, this condition can be verified that the received signal power at each UT is a constant value.

In massive MIMO systems, the size of the antenna array is small due to the placement of more antennas per unit area, and the transmitting PA is reduced accordingly. In order to make full use of the PA, the average transmit power at each

antenna should be the same. In the transmission, the average transmit power at the k -th antenna is [25]

$$P_k = \rho \cdot E \left\{ |[\mathbf{W}\mathbf{x}]_k|^2 \right\} = \rho \cdot [\mathbf{W}\mathbf{W}^H]_k. \quad (13)$$

Therefore, to ensure that the transmit power is a constant at each antenna, the constructed precoding matrix needs to satisfy the condition

$$\text{diag}(\mathbf{W}\mathbf{W}^H) = \frac{1}{M_{BS}} \mathbf{1}_{M_{BS}}. \quad (14)$$

Although the UT does not know the channel vector \mathbf{H} , it is desirable that the precoding matrix maximizes the achievable traversal rate under independent co-distributed channels. With perfect channel estimation conditions, the mutual information at the received side can be expressed as

$$I = E \left\{ \log_2 (1 + \rho \mathbf{H}^H \mathbf{W}\mathbf{W}^H \mathbf{H}) \right\}. \quad (15)$$

According to the specific formula for the traversal mutual information quantity, it is found that the traversal mutual information quantity at the UT is only related to the distribution of channel \mathbf{H} given the determined precoding matrix \mathbf{W} . The channel is assumed to be an independent identically distributed channel, i.e., $\mathbf{H} \sim \mathcal{CN}(\mathbf{0}, \mathbf{I}_{M_{BS}})$ [26]. By means of Singular Value Decomposition (SVD), this can be expressed as

$$\mathbf{W} = \mathbf{U} \begin{bmatrix} \boldsymbol{\Sigma} \\ \mathbf{0} \end{bmatrix} \mathbf{V}^H, \quad (16)$$

where \mathbf{U} and \mathbf{V} are both unitary matrices and $\boldsymbol{\Sigma}$ is a diagonal array of singular values. Since \mathbf{H} remains distribution invariant when multiplied left or right by the unitary matrix, the mutual information between the transmitter and receiver can be further expressed as

$$I = E \left\{ \log_2 \left(1 + \rho \hat{\mathbf{H}}^H \boldsymbol{\Sigma} \boldsymbol{\Sigma}^H \hat{\mathbf{H}} \right) \right\}. \quad (17)$$

Since \mathbf{U} is a unitary matrix, $\hat{\mathbf{H}} = \mathbf{U}^H \mathbf{H}$ also has the same distribution as \mathbf{H} , i.e., $\hat{\mathbf{H}} \sim \mathcal{CN}(\mathbf{0}, \mathbf{I}_{M_{BS}})$. In i.i.d. MIMO channels, the mutual information between the transmitter and receiver can reach the channel capacity only if the diagonal matrix $\boldsymbol{\Sigma}$ satisfies $\boldsymbol{\Sigma} \boldsymbol{\Sigma}^H = \frac{1}{N_{\mathbf{w}}} \mathbf{I}_{N_{\mathbf{w}}}$. Therefore, \mathbf{W} should satisfy [27]

$$\begin{aligned} \mathbf{W}^H \mathbf{W} &= \mathbf{V} \begin{bmatrix} \boldsymbol{\Sigma}^H & \mathbf{0} \end{bmatrix} \begin{bmatrix} \boldsymbol{\Sigma} \\ \mathbf{0} \end{bmatrix} \mathbf{V}^H \\ &= \frac{1}{N_{\mathbf{w}}} \mathbf{I}_{N_{\mathbf{w}}}. \end{aligned} \quad (18)$$

In summary, the precoding matrix \mathbf{W} has the following three basic conditions that need to be met

$$\begin{cases} \text{diag}(\mathbf{F}_M \mathbf{W}\mathbf{W}^H \mathbf{F}_M^H) = \frac{1}{M_{BS}} \mathbf{1}_{M_{BS}}, \\ \text{diag}(\mathbf{W}\mathbf{W}^H) = \frac{1}{M_{BS}} \mathbf{1}_{M_{BS}}, \\ \mathbf{W}^H \mathbf{W} = \frac{1}{N_{\mathbf{w}}} \mathbf{I}_{N_{\mathbf{w}}}. \end{cases} \quad (19)$$

B. Precoding Design Based on Complementary Sequences

We consider the design of the precoding matrix from the perspective of a continuous angular domain. When precoding the domain dimensions $N_{\mathbf{W}} = 2$, the precoding is $\mathbf{W} = [\mathbf{w}_1, \mathbf{w}_2]$, $\mathbf{w}_1 = [w_{1,0}, w_{1,1}, \dots, w_{1,M_{BS}-1}]^T$, $\mathbf{w}_2 = [w_{2,0}, w_{2,1}, \dots, w_{2,M_{BS}-1}]^T$. The average transmit power corresponding to the angular domains is

$$P(\omega) = \frac{\rho}{M_{BS}} \cdot \left\{ |\mathbf{w}_1|^2 + |\mathbf{w}_2|^2 + 2 \sum_{k=1}^{M_{BS}-1} \Re \left(e^{-jk\omega} (C_{\mathbf{w}_1}(k) + C_{\mathbf{w}_2}(k)) \right) \right\}, \quad (20)$$

where $C_{\mathbf{w}}(k)$ is the acyclic autocorrelation function of the vector \mathbf{w} defined by

$$C_{\mathbf{w}}(k) = \sum_{m=0}^{M_{BS}-1-k} w_m^* w_{m+k}. \quad (21)$$

To make $P(\omega)$ independent of ω , the omnidirectional transport condition is weakened to

$$C_{\mathbf{w}}(k) = 0, k \in 0, 1, \dots, M_{BS} - 1, \quad (22)$$

which is coincided with the definition of the CS.

The definition of the CS is:

$\mathbf{a} = (a_0, a_1, \dots, a_{N-1})$ and $\mathbf{b} = (b_0, b_1, \dots, b_{N-1})$ are two sequences of length N with $a_k, b_k \in \{-1, +1\}$, $k \in 0, 1, \dots, N - 1$. Their acyclic autocorrelation functions are as follows

$$\begin{aligned} C_{\mathbf{a}}(k) &= \sum_{i=0}^{N-1-k} a_i a_{i+k}, k \in 0, 1, \dots, N - 1, \\ C_{\mathbf{b}}(k) &= \sum_{i=0}^{N-1-k} b_i b_{i+k}, k \in 0, 1, \dots, N - 1. \end{aligned} \quad (23)$$

A sequence pair $\{\mathbf{a}, \mathbf{b}\}$ is called CS pair if it satisfies $C_{\mathbf{a}}(k) + C_{\mathbf{b}}(k) = 0, \forall k \neq 0$, and the sequences \mathbf{a} and \mathbf{b} are called CS.

Thus, the precoding matrix can be obtained using CS

$$\mathbf{W} = \frac{1}{\sqrt{2M_{BS}}} [\mathbf{a}, \mathbf{b}], \quad (24)$$

where \mathbf{a} and \mathbf{b} are sequences in a CS. When $N_{\mathbf{W}} = 2^n$, $M_{BS} = 2^m$ and $m > n$, a precoding matrix design similar to the above equation can be obtained by using CS

$$\mathbf{W} = \frac{1}{\sqrt{M_{BS}}} \text{diag}(\mathbf{a}) (\mathbf{1}_{M_{BS}/N_{\mathbf{w}}} \otimes \mathbf{I}_{N_{\mathbf{w}}}). \quad (25)$$

C. Construction of Complete Complementary Sequences

CCS is derived by further generalization of CS. CCS can satisfy both the properties of CS with good autocorrelation properties and individual subsequences with good intercorrelation properties between them at the same time. The set of CCS can be determined by a set of parameters (P, Q) , where P represents the number of CS in the set of CCS and Q is the length of the CCS.

$$\begin{aligned} \Omega &= \begin{pmatrix} \Psi \oplus \Psi & -\Psi \oplus \Psi \\ -\Psi \oplus \Psi & \Psi \oplus \Psi \end{pmatrix} \\ &= \left(\begin{array}{cccc|cccc|cccc} a_1 & a_1 & a_2 & a_2 & \cdots & \cdots & a_N & a_N & -a_1 & a_1 & -a_2 & a_2 & \cdots & \cdots & -a_N & a_N \\ b_1 & b_1 & b_2 & b_2 & \cdots & \cdots & b_N & b_N & -b_1 & b_1 & -b_2 & b_2 & \cdots & \cdots & -b_N & b_N \\ \hline -a_1 & a_1 & -a_2 & a_2 & \cdots & \cdots & -a_N & a_N & a_1 & a_1 & a_2 & a_2 & \cdots & \cdots & a_N & a_N \\ -b_1 & b_1 & -b_2 & b_2 & \cdots & \cdots & -b_N & b_N & b_1 & b_1 & b_2 & b_2 & \cdots & \cdots & b_N & b_N \end{array} \right) \end{aligned} \quad (30)$$

$$\Omega_{\mathbf{W}} = \begin{bmatrix} \mathbf{W}_1 \\ \mathbf{W}_2 \\ \vdots \\ \mathbf{W}_S \end{bmatrix} = \begin{bmatrix} \frac{1}{\sqrt{M_{BS}}} \text{diag}(\mathbf{C}_1) (\mathbf{1}_{M_{BS}/K} \otimes \mathbf{I}_K) \\ \frac{1}{\sqrt{M_{BS}}} \text{diag}(\mathbf{C}_2) (\mathbf{1}_{M_{BS}/K} \otimes \mathbf{I}_K) \\ \vdots \\ \frac{1}{\sqrt{M_{BS}}} \text{diag}(\mathbf{C}_S) (\mathbf{1}_{M_{BS}/K} \otimes \mathbf{I}_K) \end{bmatrix} \quad (31)$$

We generate CCS by the recursive generation method, i.e., by using a CS of shorter length to perform a splicing operation to obtain multiple pairs of longer CS, and then performing the same operation on the longer CS to obtain more CCS of the desired length. We generate the set of CCS by means of interleaving [28].

We define Ψ to be the initial set of CCS, also known as CCS seeds:

$$\Psi = \begin{pmatrix} a_1 & a_2 & \cdots & a_N \\ b_1 & b_2 & \cdots & b_N \end{pmatrix} \quad (26)$$

and

$$-\Psi = \begin{pmatrix} -a_1 & -a_2 & \cdots & -a_N \\ -b_1 & -b_2 & \cdots & -b_N \end{pmatrix}. \quad (27)$$

Define the interleaving operation as

$$\Psi \oplus \Psi = \begin{pmatrix} a_1 & a_1 & a_2 & a_2 & \cdots & \cdots & a_N & a_N \\ b_1 & b_1 & b_2 & b_2 & \cdots & \cdots & b_N & b_N \end{pmatrix} \quad (28)$$

and

$$\begin{aligned} -\Psi \oplus \Psi &= \\ &= \begin{pmatrix} -a_1 & a_1 & -a_2 & a_2 & \cdots & \cdots & -a_N & a_N \\ -b_1 & b_1 & -b_2 & b_2 & \cdots & \cdots & -b_N & b_N \end{pmatrix}. \end{aligned} \quad (29)$$

Then, the new set of CCS Ω resulting from the interleaving operation can be expressed as (30).

In this way, the CCS can then be expanded in number by this construction method, producing a set of CCS of length $N \cdot 4^n$, where N denotes the length of the initial seed sequence and n denotes the number of interleaving.

Corresponding to the SCMA multicast system in this paper, each multicast group corresponds to a precoding matrix, and the precoding matrix of each multicast group is designed by different CSs, setting the precoding set as $\Omega_{\mathbf{W}}$ in (31), where $\mathbf{C}_i = [C_i^1, C_i^2, \dots, C_i^{M_{BS}}]^T$, ($i = 1, \dots, J$) is derived from the set of CCS constructed from multiple interleaving operations.

IV. IMPLEMENTATION OF THE CS-BASED AND CCS-BASED PRECODING IN SCMA MULTICAST SYSTEM

In the SCMA multi-cell multicast system, it is assumed that J multicast groups share K orthogonal time-frequency resources, the codebook size is M and the number of users in the m -th multicast group is J_m . At the transmitter, a data stream of $\log_2 M$ bits in length is mapped directly to K -dimensional complex symbols via a predefined codebook, where M is the codebook size and K orthogonal resources on K -dimensional symbols as shown in Fig.3. Without loss of generality, it is assumed that one SCMA block contains J codebooks and that a multicast group occupies one codebook. For a multicast group, there are N independent receivers and they are randomly distributed within the cell.

Taking the SCMA multicast system with $J = 6$ multicast groups and $K = 4$ resources as an example, the resource sharing structure of SCMA can be expressed by a $K \times J$ indicator matrix

$$\mathbf{F}_{(4,6)} = \begin{bmatrix} 0 & 1 & 1 & 0 & 1 & 0 \\ 1 & 0 & 1 & 0 & 0 & 1 \\ 0 & 1 & 0 & 1 & 0 & 1 \\ 1 & 0 & 0 & 1 & 1 & 0 \end{bmatrix}, \quad (32)$$

where the rows represent resources and columns represent multicast groups. Each resource is shared by three multicast groups, and each multicast group occupies two resources. In this way, the number of multicast groups superimposed on each resource is limited, and multicast group information would not be distributed on all resources, reducing interference between user groups.

We assume that all users are time-synchronized. Therefore, at a certain time, the signal received by the i -th user in the j -th user group is the superimposed signal of all users, which can be expressed as

$$\begin{aligned} \mathbf{y} &= \underbrace{\text{diag}(\mathbf{H}_{(i,j),j} \mathbf{W}_j)}_{\text{signal to be decoded}} \mathbf{x}_j \\ &+ \underbrace{\sum_{m \neq j}^J \text{diag}(\mathbf{H}_{(i,j),m} \mathbf{W}_m)}_{\text{intra-group interference}} \mathbf{x}_m + \mathbf{n}, \end{aligned} \quad (33)$$

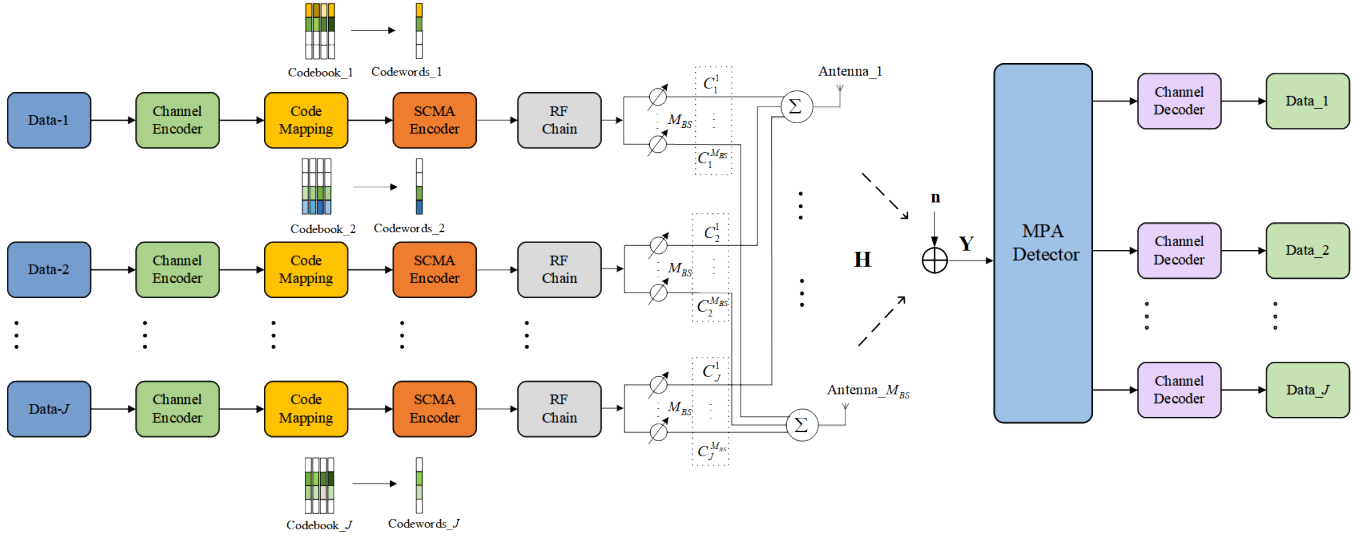


Fig. 3. SCMA Multicast System Based on CCS.

where $\mathbf{x}_j = [x_j^1, x_j^2, \dots, x_j^K]^T \in \mathbb{C}^{K \times 1}$ represents the codeword of the j -th multicast group spanning over the K resources and $\mathbf{H}_{(i,j),j} = [H_{(i,j),j}^1, H_{(i,j),j}^2, \dots, H_{(i,j),j}^{M_{BS}}]^T \in \mathbb{C}^{M_{BS} \times 1}$ represents the associated channel gain vector, $\mathbf{W}_j \in \mathbb{C}^{M_{BS} \times K}$ represents the precoding matrix of the j -th multicast group, J_m represent the number of users in m -th multicast group, $\mathbf{n} \sim \mathcal{CN}(0, \sigma^2 \mathbf{I}_K)$ is the complex Gaussian noise. In (33), the first term denotes the i -th user's signal in the j -th multicast group, and the second term represents the inter-group interference from users served by other multicast groups.

In the next, we show how to use CS and CCS to construct precoding matrix. For the proposed CS-based scheme, all multicast groups are precoded by the same CS as the precoding vector. Considering the simplest CS, we have $\mathbf{m} = (+1, +1)$ and $\mathbf{n} = (+1, -1)$. After inverting both \mathbf{m} and \mathbf{n} , $-\mathbf{m} = (-1, -1)$ and $-\mathbf{n} = (-1, +1)$ are still CS. After splicing $\mathbf{m}|\mathbf{n}$ and $\mathbf{m}|(-\mathbf{n})$, $\mathbf{m}' = (+1, +1, +1, -1)$ and $\mathbf{n}' = (+1, +1, -1, +1)$ form two new CS, which are two times as long as the original. After several iterations, we obtain the CS corresponding to the number of antennas M_{BS} . Then $N_{\mathbf{W}} = K$ and substituting CS as the initial sequence \mathbf{a} in (25), the CS-based precoding matrix can be constructed. We next show that an precoding matrix can also be constructed using CCS. For the proposed CCS-based scheme, all multicast user groups are precoded by different CSs as the precoding vector, and these different CSs are obtained from CCS in (31).

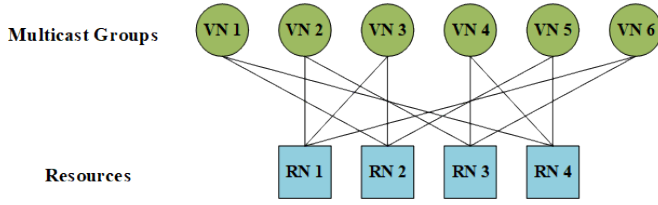
In massive MIMO systems, the larger number of antennas on the BS will inevitably lead to a larger pilot cost. When using downlink channel estimation to obtain channel state information, the pilot length must be no less than the number of BS antennas. In the precoding based SCMA multicast transmission we proposed, the user does not need to estimate the actual channel $\mathbf{H}_{(i,j),j}$ and $\mathbf{H}_{(i,j),m}$, but only requires to estimate the effective channel $\mathbf{W}_j^H \mathbf{H}_{(i,j),j}$ and $\mathbf{W}_m^H \mathbf{H}_{(i,j),m}$, and then decodes the codeword \mathbf{x}_j . Therefore, the length of each multicast group pilots can be reduced to K , which is the dimension of $\mathbf{W}_j^H \mathbf{H}_{(i,j),j}$. The user just needs to estimate

the virtual channel vectors, which are similar to the traditional small-scale MIMO system. Hence the downlink pilot overhead can be reduced significantly. However, the value of K cannot be infinitely small, because another physical meaning of K is the number of orthogonal time-frequency resources. Another role of precoding \mathbf{W}_j is to achieve a mapping between the number of BS antennas and the number of orthogonal time-frequency resources in the SCMA system. In the following decoding process, $h_{k,j}$ refers to corresponding values in the effective channel matrix.

MPA is commonly used to perform the multi-user detection in SCMA [29]. MPA is a near optimal and an iterative detection algorithm based on a bipartite factor graph modeling the receiver as illustrated in Fig. 4. Fig.4 contains two different types of nodes: resource nodes (RNs), representing the K orthogonal resources, and variable nodes (VNs), representing the J active multicast groups. MPA aims at estimating the transmitted codeword $\hat{\mathbf{x}}_j$ given the received signal \mathbf{y} observation with a computing complexity compared to the optimal maximum a posteriori decoding algorithm. Given the received signal and the channel matrix acquired at the receiver side, the maximum posteriori estimate of the superimposed codeword is [30]

$$\begin{aligned} \hat{\mathbf{x}}_j &= \arg \max_{\mathbf{a} \in \mathcal{X}} \sum_{\substack{\{\mathbf{x}_i\} \in \mathcal{X}^J \\ \mathbf{x}_j = \mathbf{a}}} P(\mathbf{x}_1, \dots, \mathbf{x}_J | \mathbf{y}) \\ &= \arg \max_{\mathbf{a} \in \mathcal{X}} \sum_{\substack{\{\mathbf{x}_i\} \in \mathcal{X}^J \\ \mathbf{x}_j = \mathbf{a}}} \prod_{i=1}^J P(\mathbf{x}_i) \prod_{k \in \mathcal{R}(j)} P(y_k | \mathbf{x}_l, l \in \mathcal{N}(k)), \end{aligned} \quad (34)$$

where $\{\mathbf{x}_i\}$ refers to the set of corresponding codewords, and \mathcal{X} represents the j -th codebook with $|\mathcal{X}| = M$ and \mathcal{X}^J is the set of codebooks of J multicast groups. The received signal at the k -th resource can be expressed as y_k . $\mathcal{N}(k) = \{j | x_{kj} \neq 0\}$ and $\mathcal{R}(j) = \{k | x_{kj} \neq 0\}$ respectively denote the set of multicast groups transmitting on RN k and the set of RN.


 Fig. 4. An SCMA factor graph with $J = 6$, $K = 4$.

The MPA process is defined as follows.

Step 1: Initialization

In the MPA detector, it is assumed that the code words sent by each user have equal probability distribution [29]. Hence, the prior probability of having sent codeword \mathbf{x}_j is uniform

$$G_{j \rightarrow k}^0(\mathbf{x}_j) = P(\mathbf{x}_j) = \frac{1}{M}, \forall j = 1, \dots, J, \forall k \in \mathcal{R}(j). \quad (35)$$

For ease of notation, we define $G_{j \rightarrow k}^0(\mathbf{x}_j)$ as the probability that user node $\text{VN } j$ transfers codeword information to resource node $\text{RN } k$ during the 0-th iteration.

Step 2: Update of information

Step 2 consists of two main sub-steps: passing information from RNs to VNs and information exchange from VNs to RNs. Let $M_{k \rightarrow j}^t(\mathbf{x}_j)$ be the extrinsic information sent from $\text{RN } k$ to $\text{VN } j$ for the corresponding codeword \mathbf{x}_j at the t -th iteration. Similarly, $M_{j \rightarrow k}^t(\mathbf{x}_j)$ is the extrinsic information passed from $\text{VN } j$ to $\text{RN } k$ for the corresponding codeword \mathbf{x}_j at the t -th iteration.

The passed message from RN_k to VN_j during the t -th iteration is given as [31]:

$$M_{k \rightarrow j}^t(\mathbf{x}_j) = \sum_{\{\mathbf{x}_i | i \in \mathcal{N}(k) \setminus j\}} \exp \left\{ -\frac{1}{\sigma^2} \left\| y_k - \sum_{\substack{j \\ x_{kj} \neq 0}} h_{kj} x_{kj} \right\|^2 \right\} \times \prod_{\{i \in \mathcal{N}(k) \setminus j\}} G_{i \rightarrow k}^{(t-1)}(\mathbf{x}_i), \quad (36)$$

where $i \in \mathcal{N}(k) \setminus j$ represents all elements in $\mathcal{N}(k)$ except j .

Next, the transmitted message from $\text{VN } j$ to $\text{RN } k$ during the same iteration is modified as:

$$M_{j \rightarrow k}^t(\mathbf{x}_j) = \frac{1}{M} \prod_{\{i \in \mathcal{R}(j) \setminus k\}} M_{i \rightarrow j}^{t-1}(\mathbf{x}_j). \quad (37)$$

To ensure that the sum of all codewords probabilities is equal to one, it is necessary to normalize the message:

$$G_{j \rightarrow k}^t(\mathbf{x}_j) = \frac{\prod_{\{i \in \mathcal{R}(j) \setminus k\}} M_{i \rightarrow j}^{t-1}(\mathbf{x}_j)}{\sum_{\mathbf{x}_j} \prod_{\{i \in \mathcal{R}(j) \setminus k\}} M_{i \rightarrow j}^{t-1}(\mathbf{x}_j)}. \quad (38)$$

Step 3: LLR calculation and bits estimation

The algorithm needs to iterate sufficiently, i.e., T iterations let's say, to converge. Then, the a posteriori probability for the corresponding codeword \mathbf{x}_j , defined as $\Pr(\mathbf{x}_j)$, is represented as:

$$\Pr(\mathbf{x}_j) = \frac{1}{M} \prod_{k \in \mathcal{R}(j)} M_{k \rightarrow j}^T(\mathbf{x}_j). \quad (39)$$

The binary log-likelihood ratio (LLR) to decide the $\log_2(M)$ bits is [31]:

$$\text{LLR}(b_i) = \log \frac{\sum_{\{\mathbf{x}_j \in \mathcal{X} | b_i = 0\}} \Pr(\mathbf{x}_j)}{\sum_{\{\mathbf{x}_j \in \mathcal{X} | b_i = 1\}} \Pr(\mathbf{x}_j)}. \quad (40)$$

Afterwards, each user bit, \hat{b}_i with $i \in \{1, \dots, \log_2(M)\}$, is estimated by comparing bit-wise LLR to 0 such that:

$$\begin{cases} \hat{b}_i = 1, & \text{LLR} \leq 0, \\ \hat{b}_i = 0, & \text{otherwise.} \end{cases} \quad (41)$$

The algorithm repeats until the maximum number of iteration is reached, and then execute the decision output.

V. NUMERICAL RESULTS

In this section, we present numerical simulations to evaluate the performance of the proposed CCS-based precoding for public information transmission in an SCMA multicast system. The BS uses a ULA array with antenna spacing $d = \lambda/\sqrt{3}$. We assume that the radius of the cell is $R = 100m$. The BS of each cell randomly selects four users for one multicast communication round. Each user is equipped with a single antenna. We construct the CCS-based precoding matrix by utilizing (6,64)-CCS in Table I, where $P = 6$ and $Q = 64$. Specific simulation parameters are shown in Table II. In Fig. 5, 6, and 7, SCMA system adopts the codebook (6,4) of Table A in APPENDIX. In the experiment in Fig. 8, the SCMA systems use the codebook(6,4), codebook(9,6) and codebook(16,8) in the APPENDIX. The effective channel is assumed to be estimated perfectly in the simulation.

TABLE I
(6,64)-COMPLETE COMPLEMENTARY SEQUENCES

Index	C	Value
1	$C_1^1, C_1^2, \dots, C_1^{64}$	+1 +1 -1 +1 +1 -1 +1 -1 -1 +1 -1 +1 -1 +1 +1 -1 -1 +1 +1 -1 +1 -1 -1 +1 -1 +1 -1 +1 -1 -1 +1 -1 -1 -1 +1 -1 +1 +1 -1 -1 +1 -1 +1 +1 -1 +1 +1 +1 -1 -1 -1 +1 -1 +1 -1 +1
2	$C_2^1, C_2^2, \dots, C_2^{64}$	+1 -1 -1 -1 +1 -1 -1 -1 +1 +1 +1 -1 -1 -1 +1 -1 -1 -1 +1 -1 -1 -1 +1 +1 +1 -1 -1 -1 -1 +1 +1 +1 -1 +1 +1 +1 -1 -1 -1 -1 +1 +1 +1 -1 -1 -1 +1 -1 -1 -1 +1 +1 +1 -1 -1 -1
3	$C_3^1, C_3^2, \dots, C_3^{64}$	-1 +1 +1 -1 +1 -1 +1 +1 -1 -1 -1 -1 +1 +1 -1 +1 +1 -1 +1 +1 +1 -1 -1 -1 -1 +1 +1 +1 -1 -1 -1 +1 -1 -1 -1 +1 +1 +1 -1 -1 -1 -1 +1 +1 +1 -1 +1 +1 +1 -1 -1 -1 -1 +1 +1
4	$C_4^1, C_4^2, \dots, C_4^{64}$	-1 -1 +1 -1 -1 +1 -1 +1 -1 +1 -1 -1 +1 -1 -1 -1 +1 -1 -1 +1 -1 +1 -1 +1 -1 -1 +1 -1 +1 +1 -1 +1 +1 -1 +1 -1 -1 +1 -1 +1 -1 +1 -1 -1 +1 -1 -1 +1 -1 +1 -1 +1 -1 -1 +1 -1
5	$C_5^1, C_5^2, \dots, C_5^{64}$	-1 -1 +1 -1 +1 -1 +1 +1 -1 -1 +1 +1 -1 +1 -1 -1 +1 -1 +1 -1 +1 +1 -1 -1 +1 +1 -1 +1 +1 +1 -1 +1 -1 -1 -1 -1 -1 -1 -1 -1 +1 -1 -1 -1 +1 -1 +1 -1 +1 +1 -1 -1 +1 +1 -1 +1
6	$C_6^1, C_6^2, \dots, C_6^{64}$	-1 +1 +1 +1 +1 -1 -1 -1 +1 -1 -1 -1 -1 -1 +1 -1 -1 -1 +1 +1 -1 +1 +1 -1 +1 +1 +1 -1 +1 +1 +1 -1 -1 -1 -1 +1 -1 -1 -1 -1 -1

TABLE II
SIMULATION PARAMETERS

Parameter Name	Value
Antenna Array	ULA
Sectors in Cell	3
Array Interval	$\lambda/\sqrt{3}$
PAS	truncated Gaussian distribution
User Distribution	Random distribution
SNR	0dB, 5dB, 10dB, 15dB, 20dB
Number of Antennas	32, 64, 128
Cell Radius	100m
Number of Users in Group	4

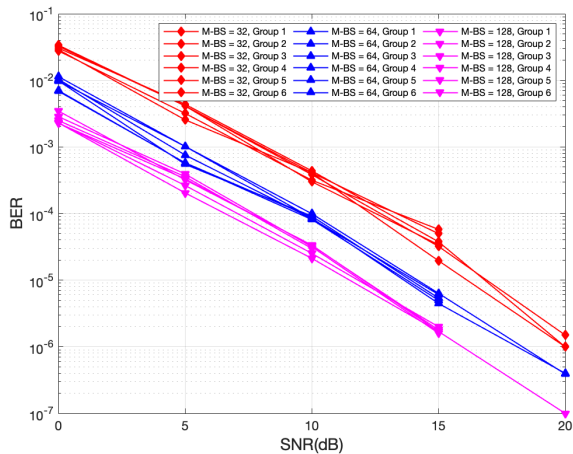


Fig. 5. BER performance comparison between different BS antenna numbers.

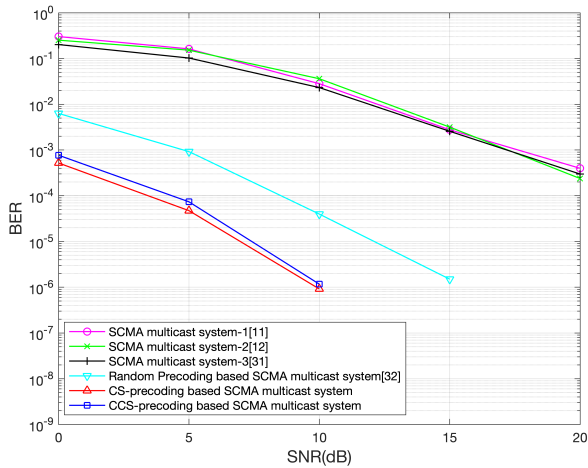
Fig.5 evaluates the BER performance with the number of BS antennas under the Rayleigh channels. In the simulation, we assume the BS with different $M_{BS} = 32, 64$ and 128 serves $J = 6$ multicast groups. And each multicast group includes four users. We can observe from the figure that the BER performance of the proposed multicast precoding becomes better when the number of BS antennas becomes large. This is due to the increase in both the number of BS antennas and the length of the complementary sequence coding. Furthermore, although this multicast precoding is proposed based on a massive MIMO system, it works relatively well even for a not very large number of BS antennas. We know that massive MIMO can deploy more antennas in the BS with the help of millimeter wave, but due to hardware limitations, this antenna cannot be infinitesimal, the number of BS antennas cannot be infinite, the suitable number of antennas of Massive MIMO usually be 128.

Fig.6 illustrates the BER achieved by SCMA multicast system [11], [12], [31], Random Precoding (e.g., using a pseudo-random binary sequence) [32], CS-based Precoding and CCS-based Precoding scheme in single-cell and multi-cell scenarios. In the case of SCMA multicast systems [11], the STBC-based SCMA system downlink transmission is designed in combination with MIMO to fully utilize the spatial domain resources thus improving the system performance without correspondingly increasing the spectrum resources. Due to

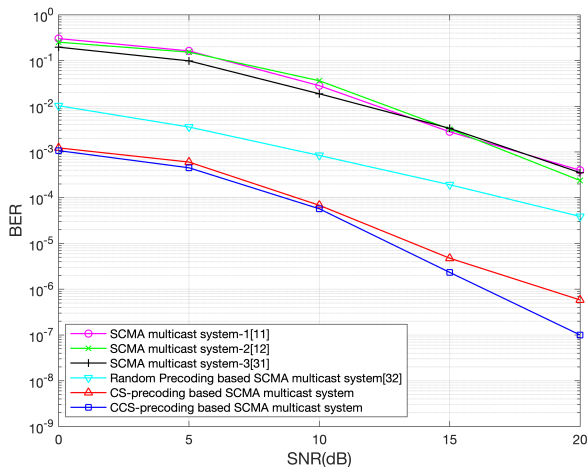
the diversity gain of multiple antennas, it has better BER performance than the conventional SCMA-based schemes. However, due to the limitations of combining STBC and MIMO, this scheme is more suitable for the case where the antennas are two at both the BS and the user, which leads to an unsatisfactory performance when the number of antennas increases, especially in massive MIMO scenarios. In the case of SCMA multicast systems [12], which is a multicast downlink transmission scheme based on MSTBC-MIMO-SCMA, it can theoretically achieve a better BER performance than that of STBC-MIMO-OFDM. However, the MSTBC-MIMO-SCMA scheme does not take into account the complex transmission environment where multiple user groups interfere with each other under multicast transmission. In the SCMA multicast system [31], a low-complexity receiving design is investigated at the receiver side to cope with the increase in the number of users. The SCMA multicast system proposed in this paper is based on the work [31] and then CS-based and CCS-based precoding are applied based on it.

The Fig.6(a) shows the BER performance of the four different precoding schemes in single-cell multicast environment. The number of BS antennas is $M_{BS} = 64$. We observe that the BER of the SCMA single-cell multicast system can be improved significantly if we exploit the CS-based Precoding and the CCS-based Precoding. It can also be inferred from the Fig.6(a) that CS-based scheme performs better than CCS-based scheme in single-cell environment. In the single-cell model, if the transmission scheme is based on CS precoding, the BS adopted precoding vector is based on the same CS in each time slot. And if the transmission scheme is based on CCS precoding, the BS adopted precoding vector is based on different CSs from the set of CCS in each time slot. Applying the CCS-based precoding transmission scheme in single-cell model not only increase complexity for BS, but also has a destabilizing effect on BER results. Therefore, in the single-cell mode, considering the complexity of the transmitter and the stability of the receiver, we believe that the CS-based precoding scheme is more advantageous. In the single-cell model, if the transmission scheme is based on CS precoding, the BS adopted precoding vector is based on the same CS in each time slot. And if the transmission scheme is based on CCS-based precoding, the BS adopted precoding vector is based on different CSs from the set of CCS in each time slot. Applying the CCS-based precoding transmission scheme in single-cell model not only increase complexity for BS, but also has a destabilizing effect on BER results. The Fig.6(b) shows the BER performance of the four different precoding schemes in multi-cell multicast environment. The number of BS antennas is $M_{BS} = 64$. As expected, we also observe from the Fig.6(b) that CCS-based scheme is superior to CS-based scheme in multi-cell scenario. Owing to the nature of the CCS have such cross-correlation characteristics: each subsequence is complementary and has good autocorrelation characteristics, and each subsequence should have good cross-correlation characteristics at the same time, the multicast group in the same time slot can use these cross-correlation characteristics to eliminate the interference between groups.

Fig.7 evaluates the BER performance of the precoding



(a)



(b)

Fig. 6. BER performance comparison between different designs in two environments. (a) single-cell. (b) multi-cell.

method we proposed with different multiplexing technologies. As a special case of multi-cell model, the single-cell model does not consider the interference between user groups, and the influence of different multiplexing technology on its trend is similar to that of multi-cell model. Therefore, we only show the results under the multi-cell model. NOMA is less sensitive than OMA to delays or errors in channel-related information feedback from the client, resulting in more robust system performance. Our simulation results also prove that SCMA and Power Domain NOMA (PD-NOMA) have lower BER than Time Division Multiple Access (TDMA) under the same experimental conditions. Besides, in order to ensure the fairness of users, the traditional PD-NOMA allocates more power to users with poor channel conditions. However, it does not strictly guarantee the quality of service expected by every user. As a mature NOMA technology, SCMA's system performance is more stable, so it can achieve better BER performance.

In Fig.8, we present the result of BER performance of the

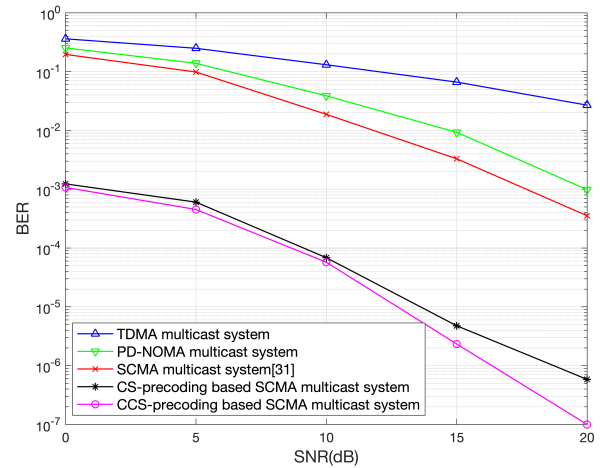


Fig. 7. BER performance comparison between different multiplexing technologies.

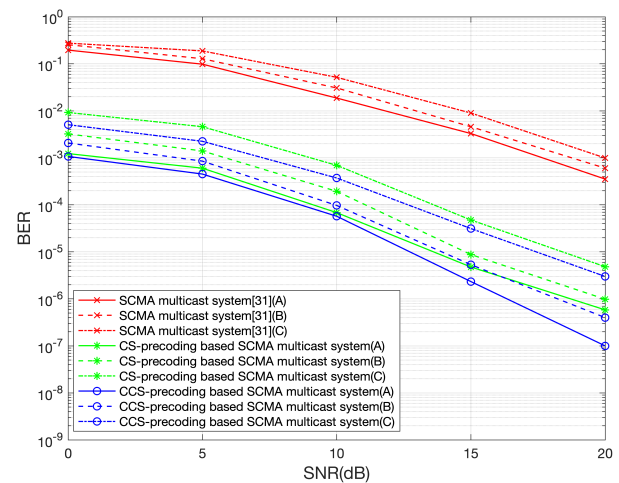


Fig. 8. BER performance of different overloading factors.

 TABLE III
 PARAMETERS OF DIFFERENT SIMULATION SCENARIOS

Scenario	(J, K)	Overloading factor
(A)	(6, 4)	150%
(B)	(9, 6)	150%
(C)	(16, 8)	200%

proposed CS-based and CCS-based precoding transmission in multi-cell for the scenarios in Table III. When SCMA is used, codebook design could be flexible according to the given overloading factor for the system. It can be observed from the Fig. 8 that the larger the overload factor is, the worse the BER performance is. The experiment also confirmed that under the same overloading factor, the increase of the number of user groups also leads to the increase of BER.

Fig.9 and Fig.10 verify the ability of omnidirectional transmission of the proposed transmission method based on complementary sequence precoding in a multicast system.

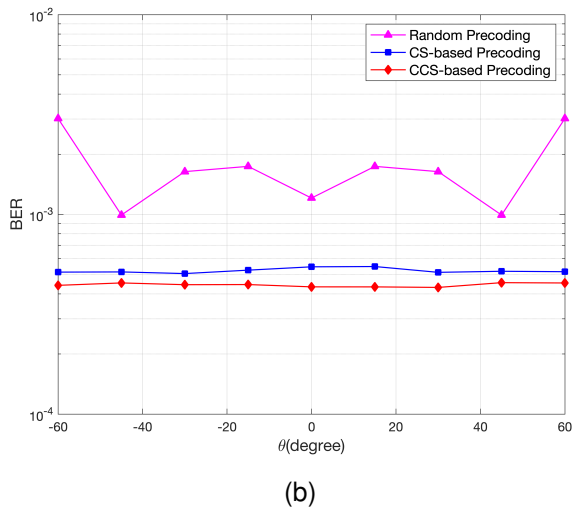
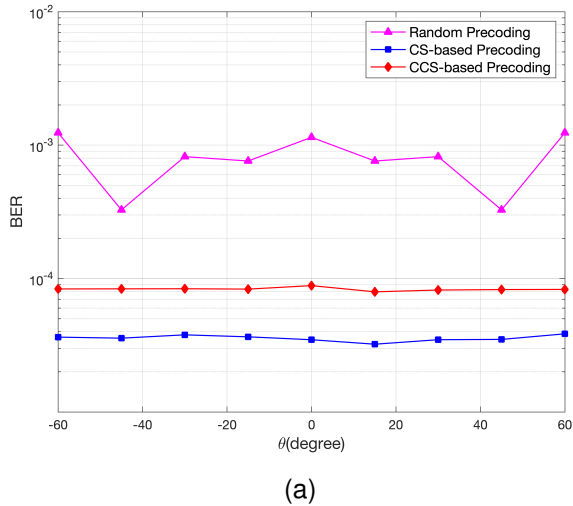


Fig. 9. BER performance comparison between different value of θ . (a) single-cell. (b) multi-cell.

An intuitive consideration is to prove the BER performance can keep constant by changing the θ between the user and the ULA array when the distance between the BS and the UT is fixed. Fig.9 shows the simulation values when the number of BS antennas $M_{BS} = 64$ and SNR = 5dB in two scenarios. We observe that the proposed CS-based precoding and CCS-based precoding exhibit constant BER performance for different values of θ in single-cell and multi-cell scenarios. For comparison, we use random precoding matrix (a pseudo-random binary sequence as the precoding vector) and the corresponding BER performance is not constant as the θ changes.

From another perspective, we examine that the transmit power is independent of ω . Fig. 10 shows that both the CS-based and CCS-based precoding can keep constant transmission power $P(\omega)$ for different values of ω . As a comparison, if the equal transmit power criterion is not satisfied, the corresponding transmit power may not be constant with respect to ω when we use other random sequence as the precoding vector, e.g., using a pseudo-random binary sequence. As a

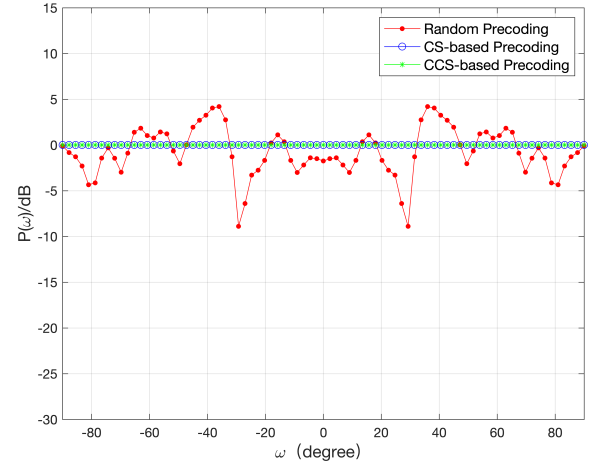


Fig. 10. $N_W = 2$, omni-directional performance of different precoding designs.

final remark, the proposed CS-based and CCS-based scheme can show superior omnidirectional transmission performance.

VI. CONCLUSION

In this paper, a precoding design based on complementary sequences for the downlink of SCMA multicast system has been proposed to reduce inter-transmitter interference. It has been theoretically proved that the proposed CS-based precoding scheme and CCS-based precoding scheme could significantly reduce the BER when the number of BS antennas is large. Furthermore, the simulation results of the proposed CCS-based precoding scheme have demonstrated the performance gain of the proposed precoding scheme when compared with other existing benchmarks for a multi-cell SCMA multicast system.

APPENDIX

The performance of the SCMA systems highly depends on the applied codebooks, we offer the codebooks which are utilized in the simulation.

First, we present the SCMA codebooks where $K = 4$, $J = 6$. The overloading factor is $J/K = 150\%$. The codebook(6,4) is shown as below.

- [13] Y. Du, B. Dong, Z. Chen, P. Gao and J. Fang, "Joint Sparse Graph-Detector Design for Downlink MIMO-SCMA Systems," in *IEEE Wireless Commun. Lett.*, vol. 6, no. 1, pp. 14-17, Feb. 2017.
- [14] W. Yuan, N. Wu, Q. Guo, Y. Li, C. Xing and J. Kuang, "Iterative Receivers for Downlink MIMO-SCMA: Message Passing and Distributed Cooperative Detection," in *IEEE Trans. Wireless Commun.*, vol. 17, no. 5, pp. 3444-3458, May 2018.
- [15] X. Chen, F.-K. Gong, G. Li and H. Ding, "Interference Subspace Alignment in Multiple-Multicast Networks," in *IEEE Trans. Veh. Technol.*, vol. 68, no. 9, pp. 8853-8865, Sept. 2019, doi: 10.1109/TVT.2019.2929475.
- [16] D. Wang and X. Wang, "An interference management scheme for Device-to-Device multicast in spectrum sharing hybrid network," *2013 IEEE 24th Annual Int. Conf. Symp. Personal, Indoor, and Mobile Radio Communications (PIMRC 2013)*, 2013, pp. 3213-3217, doi: 10.1109/PIMRC.2013.6666700.
- [17] J. Nightingale, P. Salva-Garcia, J. M. A. Calero and Q. Wang, "5G-QoE: QoE Modelling for Ultra-HD Video Streaming in 5G Networks," in *IEEE Trans. Broadcast.*, vol. 64, no. 2, pp. 621-634, June 2018, doi: 10.1109/TBC.2018.2816786.
- [18] Y. Zhang, X. Wang, D. Wang, Y. Zhang and Y. Lan, "BER Performance of Multicast SCMA Systems," in *IEEE Wireless Commun. Lett.*, vol. 8, no. 4, pp. 1073-1076, Aug. 2019.
- [19] Y. Zhang and L. Zhang, "Resource Allocation for SCMA-Based IoT Systems With Layered Multicast," in *IEEE Access*, vol. 9, pp. 144776-144785, 2021.
- [20] H. Q. Ngo, E. G. Larsson and T. L. Marzetta, "Energy and Spectral Efficiency of Very Large Multiuser MIMO Systems," in *IEEE Trans. Commun.*, vol. 61, no. 4, pp. 1436-1449, April 2013, doi: 10.1109/TCOMM.2013.020413.110848.
- [21] A. Adhikary, J. Nam, J. Ahn and G. Caire, "Joint Spatial Division and Multiplexing—The Large-Scale Array Regime," in *IEEE Trans. Inf. Theory*, vol. 59, no. 10, pp. 6441-6463, Oct. 2013, doi: 10.1109/TIT.2013.2269476.
- [22] A. Lu, X. Gao and C. Xiao, "Free Deterministic Equivalents for the Analysis of MIMO Multiple Access Channel," in *IEEE Trans. Inf. Theory*, vol. 62, no. 8, pp. 4604-4629, Aug. 2016, doi: 10.1109/TIT.2016.2573309.
- [23] C. Wen, S. Jin, K. Wong, J. Chen and P. Ting, "Channel Estimation for Massive MIMO Using Gaussian-Mixture Bayesian Learning," in *IEEE Trans. Wireless Commun.*, vol. 14, no. 3, pp. 1356-1368, March 2015, doi: 10.1109/TWC.2014.2365813.
- [24] You, L., Chen, X., Wang, W., Gao, X., "Coordinated Multicast Precoding for Multi-Cell Massive MIMO Transmission Exploiting Statistical Channel State Information," in *Electronics* 2018, 7, 338.
- [25] X. Yang, W. Jiang and B. Vucetic, "A Random Beamforming Technique for Omnidirectional Coverage in Multiple-Antenna Systems," in *IEEE Trans. Veh. Technol.*, vol. 62, no. 3, pp. 1420-1425, March 2013, doi: 10.1109/TVT.2012.2230201.
- [26] H. Q. Ngo, E. G. Larsson and T. L. Marzetta, "The Multicell Multiuser MIMO Uplink with Very Large Antenna Arrays and a Finite-Dimensional Channel," in *IEEE Trans. Commun.*, vol. 61, no. 6, pp. 2350-2361, June 2013, doi: 10.1109/TCOMM.2013.032713.120408.
- [27] L. Liu and J. Chamberland, "On the effective capacities of multiple-antenna Gaussian channels," in *Proc. IEEE Int. Symp. Inf. Theory*, 2008, pp. 2583-2587, doi: 10.1109/ISIT.2008.4595458.
- [28] Soltanian M, Naghsh M M, Stoica P. "Fast Communication: A Fast Algorithm for Designing Complementary Sets of Sequences", in *Signal Processing*, 2013, 93(7):2096-2102.
- [29] F. R. Kschischang, B. J. Frey and H. - Loeliger, "Factor graphs and the sum-product algorithm," in *IEEE Trans. Inf. Theory*, vol. 47, no. 2, pp. 498-519, Feb 2001, doi: 10.1109/18.910572.
- [30] Z. Hou, Z. Xiang, P. Ren and B. Cao, "SCMA Codebook Design Based on Divided Extended Mother Codebook," in *IEEE Access*, vol. 9, pp. 71563-71576, 2021, doi: 10.1109/ACCESS.2021.3078568.
- [31] S. Li, Y. Feng, Y. Sun and Z. Xia, "A Low-Complexity Detector for Uplink SCMA by Exploiting Dynamical Superior User Removal Algorithm," in *Electronics*, 2022, 1-19
- [32] B. Scheers and V. Le Nir, "Pseudo-Random Binary Sequence Selection for Delay and Add Direct Sequence Spread Spectrum Modulation Scheme," in *IEEE Commun. Lett.*, vol. 14, no. 11, pp. 1002-1004, November 2010, doi: 10.1109/LCOMM.2010.100410.100906.



Shufeng Li received the B.Sc. and M.Sc. degrees from Hebei University of technology, Hebei, China, in 2004 and 2007, and Ph.D. degree from Beihang University, Beijing, China, in 2011. He is currently an associate professor with the School of Information and Engineering, Communication University of China, Beijing, China. His research interests mainly include channel estimation, massive MIMO communication and non-orthogonal multiple access.



Xin Yu received the B.Sc. degree from Communication University of China, Beijing, China, in 2020, where she is currently pursuing the M.Sc. degree with the School of Information and Communication Engineering. Her current research interests mainly include wireless communication, multicast and non-orthogonal multiple access.



Yao Sun is currently a Lecturer with James Watt School of Engineering, the University of Glasgow, Glasgow, UK. Dr. Sun has extensive research experience in wireless communication area. He has won the IEEE Communication Society of TAOS Best Paper Award in 2019 ICC. He has been the guest editor for special issues of several international journals. He has served as TPC Chair for UCET 2021, and TPC member for number of international conferences, including GLOBECOM 2020, WCNC 2019, ICCT 2019. His research interests include intelligent wireless networking, network slicing, blockchain system, internet of things and resource management in mobile networks. Dr. Sun is a senior member of IEEE.



Libiao Jin received the B.Sc. degree from Minzu University of China in 2000, and the M.Sc. and Ph.D. degree from Communication University of China in 2003 and 2008. He is currently a professor with the School of Information and Communication Engineering, Communication University of China, Beijing, China. His research interests mainly include information network technology, wireless communication and deep learning.



Zhiping Xia received the B.Sc. and M.Sc. degrees from Communication University of China, Beijing, China, in 2000 and 2003. He is currently a professorate senior engineer with Academy of Broadcasting Science, Beijing, China. His research interests mainly include LTE based 5G broadcast, digital terrestrial television and UHF band frequency planning.